

# Variant c.2262A>C in *DOCK9* Leads to Exon Skipping in Keratoconus Family

Justyna A. Karolak,<sup>1,2</sup> Malgorzata Rydzanicz,<sup>3</sup> Barbara Ginter-Matuszewska,<sup>1,2</sup> Jose A. Pitarque,<sup>4</sup> Andrea Molinari,<sup>4</sup> Bassem A. Bejjani,<sup>5</sup> and Marzena Gajecka<sup>2,1</sup>

<sup>1</sup>Department of Genetics and Pharmaceutical Microbiology, Poznan University of Medical Sciences, Poznan, Poland

<sup>2</sup>Institute of Human Genetics, Polish Academy of Sciences, Poznan, Poland

<sup>3</sup>Department of Medical Genetics, Medical University of Warsaw, Warsaw, Poland

<sup>4</sup>Department of Ophthalmology, Hospital Metropolitano, Quito, Ecuador

<sup>5</sup>Elson S. Floyd College of Medicine, Washington State University, Spokane, Washington, United States

Correspondence: Marzena Gajecka, Institute of Human Genetics, Polish Academy of Sciences, Strzeszynska 32, Poznan, 60-479, Poland; gamar@man.poznan.pl.

Submitted: June 22, 2015

Accepted: November 5, 2015

Citation: Karolak JA, Rydzanicz M, Ginter-Matuszewska B, et al. Variant c.2262A>C in *DOCK9* leads to exon skipping in keratoconus family. *Invest Ophthalmol Vis Sci.* 2015;56:7687-7690. DOI:10.1167/iovs.15-17538

**PURPOSE.** Keratoconus (KTCN) is a degenerative disorder of the eye that is characterized by a conical shape and thinning of the cornea, resulting in impaired visual function. Previously, we identified heterozygous single base-pair substitutions in *DOCK9*, *IPO5*, and *STK24*, showing concurrent 100% segregation with the affected phenotype in an Ecuadorian family. As the pathogenic consequences of these variants were not obvious, we performed in vitro splicing analyses to determine their functional significance.

**METHODS.** We generated expression constructs using patient DNA as a template corresponding to the wild-type and mutant alleles of *DOCK9*, *IPO5*, and *STK24*. After transfecting HeLa cells with each construct, total RNA samples were extracted, reverse transcribed, and amplified using specific primers.

**RESULTS.** In vitro splicing analysis revealed that only c.2262A>C in exon 20 of *DOCK9* led to aberrant splicing, resulting in the changed ratio between two protein isoforms: a normal transcript and a transcript with exon skipping. The exon skipping causes a premature stop codon, disrupting the functional domains of *DOCK9* protein, which may alter the biological role of *DOCK9* as a *Cdc42* activator.

**CONCLUSIONS.** Based on in vitro results, we demonstrated that c.2262A>C substitution in *DOCK9*, previously identified in KTCN-affected members of an Ecuadorian family, leads to a splicing aberration. However, because the mutation effect was observed in vitro, a definitive relationship between *DOCK9* and KTCN phenotype could not be established. Our results indicate that further elucidation of the causes of KTCN is needed.

**Keywords:** keratoconus, *DOCK9*, splicing alteration, exon skipping, splicing assay, keratoconus genetics

Keratoconus (KTCN; Online Mendelian Inheritance in Man 148300) is a progressive eye disorder characterized by thinning and a conically shaped protrusion of the cornea, resulting in altered refractive powers and impairment of visual function.<sup>1</sup> Because the incidence rate of KTCN is one in 2000 individuals in the general population, its frequency makes it the most common corneal ectatic disorder.<sup>1</sup> However, the exact causes of KTCN remain unknown. While many studies have examined the environmental factors influencing the development of the disease, such as constant eye rubbing or contact lens wear, a majority of KTCN investigations have focused on the underlying genetic triggers.<sup>2,3</sup>

In 2009, we identified a linkage between KTCN and a novel locus at 13q32.<sup>4</sup> The screening of candidate genes from this region has revealed heterozygous nucleotide substitutions in exonic region of *DOCK9* (c.2262A>C) and intronic regions of *IPO5* (c.2377-132A>C) and *STK24* (c.1053+29G>C) showing concurrent 100% segregation with the affected phenotype in the large, multigenerational Ecuadorian family KTCN-014.<sup>5</sup> However, these variants have unknown biological implications. In silico analyses with different prediction algorithms showed

that variant c.2262A>C in *DOCK9* resulting in a Gln754His substitution in *DOCK9* might possibly be damaging for protein structure and function.<sup>5</sup> However, the functional consequence of this variation has not yet been explored.

In order to determine the functional significance of the identified sequence variants, we assessed the effect on splicing caused by these substitutions. Here, we demonstrate that c.2262A>C variant in exon 20 of *DOCK9* leads to an in vitro splicing defect, resulting in exon skipping.

## MATERIALS AND METHODS

The genomic variants c.2262A>C, c.2377-132A>C, and c.1053+29G>C in *DOCK9*, *IPO5*, and *STK24*, respectively, were detected previously by direct sequencing in all affected members of Ecuadorian family KTCN-014.<sup>5</sup>

The identified alterations were examined using total RNA samples extracted from lymphoblastoid cell lines derived from affected and control subjects from the KTCN-014 family. Total RNA was isolated and reverse transcribed as described

TABLE. Specific Primers Used in Experiments

Primer Name	Sequence 5'–3'	Product Size, bp
Primers specific for regions of interest in <i>DOCK9</i> , <i>IPO5</i> , and <i>STK24</i> used for DNA and cDNA amplification		
DOCK9_Fs	CACCATGTGCATTTATGGCAGACCTGG	1661, cDNA 346
DOCK9_Rs	CCTGCCCATCCCAAGCTC	
IPO5_Fs	CACCATGGTTCGAGTGGCAGCAGCGGAAT	1745, cDNA 346
IPO5_Rs	CTCATCTTGTAGTACTCTT	
STK24_Fs	CACCATGGAAACAGATGGCCAAGCC	1532, cDNA 199
STK24_Rs	CTCTGCAAACAGAGGAGAAA	
Primers specific for regions of interest in <i>DOCK9</i> , <i>IPO5</i> , and <i>STK24</i> used for quantitative expression		
DOCK9_Fq	ACCATCACAAAACCCAGAA	196
DOCK9_Rq	ACCTTCCGTCTTTCAGGAG	
IPO5_Fq	TGCCTCTTCTCCTGGAGTGT	177
IPO5_Rq	TAAGGCATCCATCTCCATT	
STK24_Fq	TCTGGGGACTGGATCTTCAC	118
STK24_Rq	AGAAAGGCCTCTTCGGGA	

previously.<sup>5</sup> Gene-specific PCRs for the tested genes *DOCK9*, *IPO5*, and *STK24* were performed using *Taq* polymerase (Sigma-Aldrich, Munich, Germany) and 0.4  $\mu$ L each cDNA sample in a final reaction volume of 25  $\mu$ L. The primers used for cDNA amplification are shown in the Table. The products were visualized under ultraviolet (UV) light on 2% agarose gel stained with ethidium bromide.

For the in vitro splicing experiments, genomic DNA samples from an affected individual (KTCN-014-16) and from an unaffected individual not carrying mutations (KTCN-014-01) were amplified using primers specific for the regions of interest in *DOCK9*, *IPO5*, and *STK24*, as shown in the Table. Polymerase chain reaction analyses were performed using *Taq* DNA polymerase in a final volume of 25  $\mu$ L (Thermo Scientific, San Jose, CA, USA). Detailed protocol and thermal conditions are available upon request. After purification with a GenElute PCR Clean-Up Kit (Sigma-Aldrich), the PCR fragments were ligated into the pTarget vector using the pTarget Mammalian Expression Vector System (Promega, Mannheim, Germany) and transformed into JM109 competent cells according to the manufacturer's protocol. The colonies containing the recombinant vectors were selected using colony PCR. The integrity of the clones was confirmed by Sanger sequencing using a BigDye Terminator v3.1 Cycle Sequencing Kit (Applied Biosystems, Inc., Foster City, CA, USA). The sequence data were analyzed using Sequencher 5.0 software (Gene Codes Corporation, Ann Arbor, MI, USA). Plasmid DNA for carrying out the transfections was extracted from overnight cultures with a GenElute HP Plasmid Maxiprep Kit (Sigma-Aldrich).

HeLa cells were transiently transfected with 2  $\mu$ g of each wild-type and mutant construct using an Escort II Transfection Kit (Sigma-Aldrich) according to the manufacturer's instructions. Total RNA was extracted from cells harvested after 48 hours of transfection using an RNeasy Mini Kit (Qiagen, Hilden, Germany). Total RNA derived from nontransfected HeLa cell lines was used as a control. Template RNA (0.3  $\mu$ g total RNA) was treated with DNase and reverse transcribed using a Maxima First Strand cDNA Synthesis Kit (Thermo Scientific).

Qualitative *DOCK9*, *IPO5*, and *STK24* expression analyses were performed using the primers shown in the Table. Gene-specific PCR reactions for the tested genes were performed using *Taq* polymerase (Sigma-Aldrich) and 0.4  $\mu$ L each cDNA sample in a final 25- $\mu$ L reaction volume. The products were visualized under UV light on 2% agarose gel stained with ethidium bromide, and the electrophoresis gels were analyzed using ImageJ ([\[imagej.nih.gov/ij/\]\(http://imagej.nih.gov/ij/\)\); provided in the public domain by the National Institutes of Health, Bethesda, MD, USA\). All PCR products were gel purified with a ZymoClean Gel DNA Recovery Kit \(Zymo Research, Irvine, CA, USA\) and sequenced using a BigDye Terminator v3.1 Cycle Sequencing Kit \(Applied Biosystems, Inc.\). The experiments were run in duplicate.](http://</a></p>
</div>
<div data-bbox=)

The quantitative expression profiles of both wild-type and mutant alleles of *DOCK9*, *IPO5*, and *STK24* were assessed using the specific primers listed in the Table. Primers B-A\_F (5'-CACCACACCTTCTACAATG-3') and B-A\_R (5'-TAGCA CAGCCTGGATAG-3') were applied to amplify the internal control  $\beta$ -actin gene. Reverse transcription-quantitative PCR (RT-qPCR) was carried out in a total volume of 10  $\mu$ L containing 5  $\mu$ L DyNAmo Color Flash SYBR Green qPCR (Thermo Scientific), 0.5  $\mu$ M each primer, and 0.1  $\mu$ g complementary DNA (cDNA). Quantitative PCR conditions included 40 cycles of 95°C for 10 seconds, 55°C for 30 seconds, and 72°C for 15 seconds. Quantification of the expression of mutated and wild-type *DOCK9*, *IPO5*, and *STK24* genes was conducted using SYBR Green assays (Thermo Scientific). Validation experiments demonstrated that the amplification efficiencies of the control and all target amplicons were nearly equal. All samples were run in triplicate. The dosage of each amplicon relative to  $\beta$ -actin and normalized to control HeLa cDNA was determined using the  $\Delta\Delta$ Ct method with a *P* value of 0.03. The acquired data were analyzed using LightCycler 96 application software (Roche Diagnostics, Penzberg, Germany).

Variants were analyzed in silico using Human Splicing Finder 3.0 (HSF; <http://www.umd.be/HSF3> [in the public domain]) to predict the effects of the variants on splicing motifs, including the acceptor and donor splice sites, the branch point, and auxiliary sequences known to either enhance or repress splicing.<sup>6</sup>

## RESULTS AND DISCUSSION

Computational-assisted analyses with the HSF tool revealed that variants c.2262A>C in *DOCK9* and c.1053+29G>C in *STK24* potentially had an impact on splicing, while the c.2377-132A>C substitution in *IPO5* was classified as a variant, which probably did not affect mRNA processing. However, it is known that in silico tools do not always predict splicing defects correctly; therefore, all calculations should be confirmed experimentally.<sup>7</sup> For this reason, in order to verify the in silico predictions, the identified alterations were examined by direct RT-PCR using

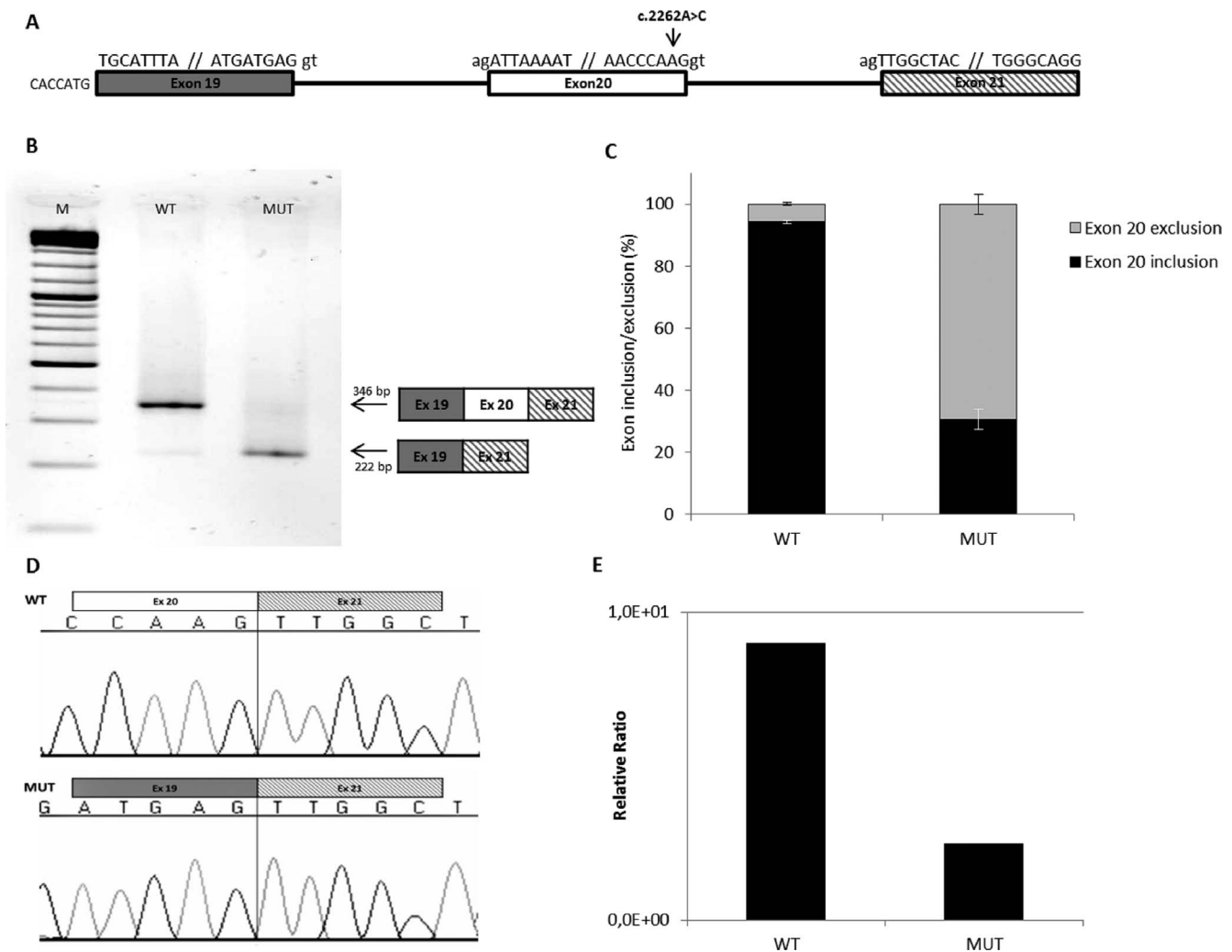


**FIGURE.** Splicing assay of *DOCK9*. **(A)** Representation of the construct designed for the c.2262A>C variant in *DOCK9*, including Kozak consensus (CACCATG) and exon (*uppercase letters*) and intron (*lowercase letters*) junction sequences. **(B)** Gel analysis of splice variants identified by RT-PCR on RNA extracted from transfected HeLa cells. WT, wild-type construct; MUT, mutated construct; M, ladder; 346 bp, normal transcript; 222 bp, aberrant transcript. **(C)** Histogram depicting the relative percentage (%) of each transcript calculated against the total intensity of the bands representing each isoform, using ImageJ. **(D)** Sequencing result of different bands obtained by PCR representing a normal product from the c.2262A allele and an aberrant product from the c.2262C allele with the exclusion of exon 20 of *DOCK9*. **(E)** Quantitative real-time PCR analysis of *DOCK9* mRNA in wild-type c.2262A and mutant c.2262C HeLa cells. Expression level was normalized to  $\beta$ -actin.

total RNA samples extracted from lymphoblastoid cell lines derived from both an affected individual and a control individual. As a result, in both subjects, we observed only the transcript representing correctly spliced mRNA (Supplementary Fig. S1). Based on the results of direct RNA analysis, we hypothesized that the absence of abnormal transcripts in mutation carrier patients might be explained by a lack of pathogenic impact of the tested variation on mRNA splicing or by a nonsense-mediated decay (NMD) pathway.<sup>8</sup> The NMD mechanism eliminates mRNAs containing premature termination codons, and thus, the aberrant transcript may be undetectable in a straightforward RNA analysis.<sup>9</sup> A similar effect was observed by Granata et al.<sup>10</sup> in a direct analysis of RNA derived from patients with variegate porphyria.

Due to the contradictory results of the computational predictions and direct RNA analysis of the processed transcripts from the patient cell lines, we performed in vitro splicing assays to definitively examine whether single base substitutions in *DOCK9*, *IPO5*, and *STK24* cause splicing aberrations. We generated expression constructs using DNA

samples as templates corresponding to the wild-type and mutant alleles of *DOCK9*, *IPO5*, and *STK24*. Forty-eight hours after transfecting the HeLa cells, the RNA samples were extracted, reverse transcribed, and amplified using specific primers, which are presented in the Table.

The splicing experiments indicated that the variants in *IPO5* and *STK24*, c.2377-132A>C, and c.1053+29G>C, respectively, produced normal transcripts, and no splicing alterations were detected (Supplementary Fig. S2). However, in the *DOCK9* analysis, we observed that the c.2262A>C variant in exon 20 generated an aberrantly spliced product. Interestingly, two amplicons of different lengths were both produced by the construct harboring the wild-type c.2262A and mutant c.2262C alleles (Figs. A, B). However, compared with the wild-type, c.2262C caused a relative change in the isoform ratio (measured using ImageJ) toward an increased level of shorter transcripts and a decreased level of normal transcripts (Fig. C).

Direct sequencing of each band showed that the 346-bp amplicon corresponds to the normal transcript containing exons 19, 20, and 21 of *DOCK9*, while the shorter amplicon,

222 bp in size, corresponds to the alternatively spliced form, resulting in skipping exon 20 (Fig. D).

Translation of the full-length *DOCK9* transcript generates a functional protein with 2070 amino acids, whereas translation of the aberrant transcript resulting from the c.2262A>C variation is predicted to produce a premature stop codon and a truncated protein with 722 amino acids. This premature translation termination codon disrupts the DHR1 domain and leads to the deletion of the DHR2 domain of *DOCK9* protein. Because these two core domains are responsible for recruitment to cellular membranes (DHR1) and specific Cdc42 activation (DHR2), their disruption might change the function of *DOCK9* due to its altered GTP/GDP exchange factor activity.<sup>11-13</sup> Quantitative real-time PCR analysis of *DOCK9* mRNA in wild-type c.2262A and mutant c.2262C HeLa cells showed a 3.63-fold lower expression of *DOCK9* in the presence of the mutation (Fig. E), suggesting that this sequence variation might be biologically significant.

While the pathogenic consequence of truncating mutations is obvious, little is still known about the pathogenicity of many single base-pair missense changes in the coding regions of genes or deep intronic substitutions. The role of these variants is difficult to evaluate, as they usually are referred to as unclassified or nonpathogenic variants. However, a fraction of them might be deleterious due to their potential impact on the splicing process.<sup>8</sup> Different strategies may be used to identify causative splicing mutations, including in silico predictions, direct analysis of patient RNA, or splicing assays.

To assess the pathogenicity of the variants identified in our KTCN patients, we used a combination of in silico tools and experimental approaches; our results indicate that these methods do not always provide concordant results. While the prediction tool revealed that variants c.2262A>C in *DOCK9* and c.1053+29G>C in *STK24* could potentially have an impact on splicing, the laboratory tests indicated that only c.2262A>C in *DOCK9* resulted in a splicing aberration. The differences between the in silico predictions and the laboratory results were not entirely unexpected, as it is known that computational tools display a considerable degree of unreliability, depending on the genes analyzed.<sup>7</sup>

In our study, c.2262A>C in *DOCK9* caused significant changes in splice patterns. Aberrant transcripts were produced in vitro in the *DOCK9* minigene assay, but not in the patient RNA derived from the lymphoblastoid cell line. High levels of agreement between the results of splicing assays and patient RNA analyses are typically observed. However, data showing differences between the results of these two approaches are also available.<sup>10,14</sup> The discrepant splice patterns might be due to cell type-specific splice profiles, differences in gene expression, or differences in genomic context.<sup>9</sup> In our research, RNA samples extracted from peripheral blood were not available; therefore, direct analyses could not be performed to further investigate this variant.

In conclusion, our in vitro studies demonstrated that genomic variant c.2262A>C in *DOCK9*, previously identified in Ecuadorian KTCN patients, altered the ratio between two protein isoforms: a normal transcript and a transcript with exon skipping. Based on the results of the bioinformatics analyses and the data regarding the structure of *DOCK9* protein, we hypothesize that the identified exon-skipping variant might disrupt the functional domains of *DOCK9* protein and alter the biological role of *DOCK9* as a Cdc42 activator. As a change in the balance between two protein isoforms is observed, the phenotypic effect is not obvious compared with the complete removal of the normal transcript. However, it is known that the relative abundance of alternatively spliced RNA isoforms can lead to diseases.<sup>15</sup>

To summarize, based on our in vitro results, we demonstrated that the c.2262A>C substitution in *DOCK9*, previously

identified in KTCN members of an Ecuadorian family, leads to a splicing aberration. However, because the effect was observed in vitro, a definitive relationship between *DOCK9* and the KTCN phenotype could not be established. Our results indicate that further elucidation of the causes of KTCN is needed.

### Acknowledgments

Supported by Polish Ministry of Science and Higher Education and National Science Centre in Poland Grants NN402591740 and 2013/10/M/NZ2/00283, and Doctoral Scholarship Etiuda 1, 2013/08/T/NZ5/00754. The authors alone are responsible for the content and writing of the paper.

Disclosure: **J.A. Karolak**, None; **M. Rydzanicz**, None; **B. Ginter-Matuszewska**, None; **J.A. Pitarque**, None; **A. Molinari**, None; **B.A. Bejjani**, None; **M. Gajecka**, None

### References

- Rabinowitz YS. Keratoconus. *Surv Ophthalmol.* 1998;42:297-319.
- Nowak DM, Gajecka M. The genetics of keratoconus. *Middle East Afr J Ophthalmol.* 2011;18:2-6.
- Abu-Amro KK, Al-Muammar AM, Kondkar AA. Genetics of keratoconus: where do we stand? *J Ophthalmol.* 2014;2014:641708.
- Gajecka M, Radhakrishna U, Winters D, et al. Localization of a gene for keratoconus to a 5.6 Mb interval on 13q32. *Invest Ophthalmol Vis Sci.* 2009;50:1531-1539.
- Czugala M, Karolak JA, Nowak DM, et al. Novel mutation and three other sequence variants segregating with phenotype at keratoconus 13q32 susceptibility locus. *Eur J Hum Genet.* 2012;4:389-397.
- Desmet FO, Hamroun D, Lalande M, Collod-Bérout G, Claustres M, Bérout C. Human Splicing Finder: an online bioinformatics tool to predict splicing signals. *Nucleic Acids Res.* 2009;37:e67.
- Hartmann L, Theiss S, Niederacher D, Schaal H. Diagnostics of pathogenic splicing mutations: does bioinformatics cover all bases? *Front Biosci.* 2008;13:3252-3272.
- Maquat LE. Nonsense-mediated mRNA decay: splicing, translation and mRNP dynamics. *Nat Rev Mol Cell Biol.* 2004;5:89-99.
- Baralle D, Lucassen A, Buratti E. Missed threads. The impact of pre-mRNA splicing defects on clinical practice. *EMBO Rep.* 2009;10:810-816.
- Granata BX, Baralle M, De Conti L, Parera V, Rossetti MV. Characterization of variegated porphyria mutations using a minigene approach. *JIMD Rep.* 2015;20:39-44.
- Kwofie MA, Skowronski J. Specific recognition of Rac2 and Cdc42 by DOCK2 and DOCK9 guanine nucleotide exchange factors. *J Biol Chem.* 2008;283:3088-3096.
- Côté J, Motoyama AB, Bush JA, Vuori K. A novel and evolutionarily conserved PtdIns(3,4,5)P3-binding domain is necessary for DOCK180 signalling. *Nat Cell Biol.* 2005;7:797-807.
- Côté JF, Vuori K. In vitro guanine nucleotide exchange activity of DHR-2/DOCKER/CZH2 domains. *Methods Enzymol.* 2006;406:41-57.
- van der Klift HM, Jansen AM, van der Steenstraten N, et al. Splicing analysis for exonic and intronic mismatch repair gene variants associated with Lynch syndrome confirms high concordance between minigene assays and patient RNA analyses. *Mol Genet Genomic Med.* 2015;3:327-345.
- Ward AJ, Cooper TA. The pathobiology of splicing. *J Pathol.* 2010;220:152-163.